

# Spin decontamination for magnetic dipolar coupling calculations: Application to high-spin molecules and solid-state spin qubits

Timur Biktagirov,<sup>1</sup> Wolf Gero Schmidt,<sup>1</sup> and Uwe Gerstmann<sup>1</sup>

<sup>1</sup>*Lehrstuhl für Theoretische Materialphysik, Universität Paderborn, 33098 Paderborn, Germany*

(Dated: May 4, 2020)

An accurate description of the two-electron density, crucial for magnetic coupling in spin systems, provides in general a major challenge for density functional theory calculations. It affects, e.g., the calculated zero-field splitting (ZFS) energies of spin qubits in semiconductors that frequently deviate significantly from experiment. In the present work (i) we propose an efficient and robust strategy to correct for spin contamination in both extended periodic and finite-size systems, (ii) verify its accuracy using model high-spin molecules, and finally (iii) apply the methodology to calculate accurate ZFS of spin qubits (NV<sup>-</sup> centers, divacancies) in diamond and silicon carbide. The approach is shown to reduce the dependence on the used exchange-correlation functional to a minimum.

An electron-electron magnetic dipolar interaction in a high-spin molecular system leads to the energy splitting of its  $m_S$  spin sublevels in the absence of external magnetic fields [1, 2]. A theoretical prediction of the magnetic dipolar coupling and the resulting zero-field splitting (ZFS) is, however, challenged by the so-called spin contamination of the two-particle spin density [3, 4]. It arises in electronic structure calculations if the spin channels are allowed to differ in spatial representation (see also Fig. 1), leading to wave functions that are not eigenfunctions of the total spin-squared operator  $S^2$  [5, 6]. In particular, it can result in non-vanishing ZFS even for infinitely large spin separation [4].

Although the effects of spin contamination are well-known for molecular systems, they have scarcely been considered for solids. This is related to the fact that the remedy typically used to correct for spin contamination in density functional theory (DFT) calculations with a localized basis set, i.e., the the unrestricted natural orbital (UNO) approach [3], cannot be straightforwardly realized in a plane-wave description of systems with periodic boundary conditions. High-spin states in solids, however, attract significant attention as potential spin qubits, i.e. building blocks of quantum technological devices. Here, the ZFS serves as an essential lever to spectroscopically address and distinguish a specific spin center among other defects present in the host material.

In the present work we propose an efficient strategy for spin decontamination in magnetic dipolar coupling driven ZFS, which is suitable for extended periodic systems. It is based on taking both the  $m_S = S$  and  $m_S = S - 1$  spin states of the system into account when calculating the spin-dipolar interaction. The approach is first demonstrated using a molecular biradical as model system and subsequently applied to rectify the calculated ZFS of the nitrogen-vacancy (NV<sup>-</sup>) [7–12], silicon-carbon divacancy (VV<sup>0</sup>) [13–18] and silicon vacancy (V<sub>Si</sub><sup>-</sup>) [19–22] centers in silicon carbide (SiC), and the NV<sup>-</sup> center in diamond [23–32]. Finally, we demonstrate that the established strategy can generally be applied for  $S \geq 1$  systems

and, moreover, is robust with respect to the exchange-correlation functional.

The phenomenological spin Hamiltonian [1]

$$\hat{H}^{\text{ZFS}} = \hat{\mathbf{S}} \cdot \mathbf{D} \cdot \hat{\mathbf{S}} \quad (1)$$

is conventionally adopted to characterize the ZFS in terms of the parameters  $D = D_{zz} - \frac{1}{2}(D_{xx} + D_{yy})$  and  $E = \frac{1}{2}(D_{yy} - D_{xx})$ , where  $D_{ii}$  are the eigenvalues of the symmetric and traceless  $3 \times 3$  tensor  $\mathbf{D}$ , and axially symmetric  $\mathbf{D}$  tensors lead to vanishing  $E$ .

Within the DFT framework, the spin-dipolar coupling driven  $\mathbf{D}$  tensor (referred to as spin-spin ZFS) is derived from the spatial distribution of Kohn-Sham orbitals obtained with standard spin-polarized self-consistent field calculations [33–37]. For the  $S \geq 1$  high-spin state of a system, the spin-spin  $\mathbf{D}$  tensor is given by

$$\mathbf{D}^{\text{SS}} = \frac{\mathbf{d}}{S(S - \frac{1}{2})}, \quad (2)$$

where the elements of the traceless  $3 \times 3$  matrix  $\mathbf{d}$  are constituted by magnetic dipolar interaction between all the pairs of occupied Kohn-Sham states  $m$  and  $n$  (with  $a, b = x, y, z$ ):

$$d_{ab} = \frac{\alpha^2}{8} \sum_{m,n} \chi_{m,n} \int \frac{|\mathbf{r} - \mathbf{r}'|^2 \delta_{ab} - 3(\mathbf{r} - \mathbf{r}')_a (\mathbf{r} - \mathbf{r}')_b}{|\mathbf{r} - \mathbf{r}'|^5} \times [n_{mm}(\mathbf{r})n_{nn}^*(\mathbf{r}') - n_{mn}(\mathbf{r})n_{mn}^*(\mathbf{r}')] d\mathbf{r}d\mathbf{r}'. \quad (3)$$

In Eq. 3,  $\alpha$  is the fine-structure constant, the charge densities  $n_{mn}(\mathbf{r}) = \psi_m(\mathbf{r})\psi_n(\mathbf{r})$  reflect the spatial distribution of the orbitals, and  $\chi_{m,n}$  originates from the matrix elements of spin-operators:  $\chi_{m,n} = 1$  when the orbital belong to the same spin channel, and  $\chi_{m,n} = -1$  otherwise. Throughout the manuscript, we will also make use of the magnetic dipolar coupling parameter  $d = d_{zz} - \frac{1}{2}(d_{xx} + d_{yy})$  analogous to the  $D$  value. Note that the expression in the square brackets in Eq. 3 is an

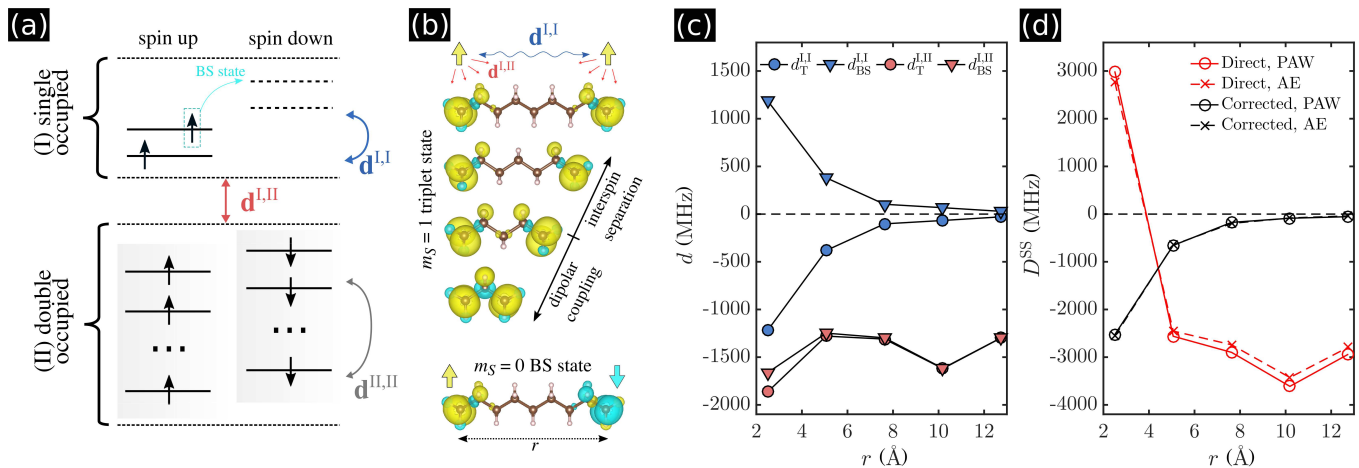


FIG. 1. (a) Schematic illustration of the electron-electron magnetic dipole interaction in a spin-triplet system. The overall coupling  $\mathbf{d}$  originates from the interaction between the two single occupied Kohn-Sham orbitals (denoted as I), as well as the contributions arising from the double occupied orbitals (II). (b) A set of biradicals of different length (general formula  $C_nH_{2n}$ ; adopted from Ref. [4]). Magnetization density in their triplet and BS states is illustrated with yellow (positive) and cyan (negative) isosurface. (c) The contributions to the magnetic dipolar coupling in the triplet ( $d_T^{I,I}$ ,  $d_T^{I,II}$ ) and BS ( $d_{BS}^{I,I}$ ,  $d_{BS}^{I,II}$ ) states of the biradicals. (d) The  $D^{SS}$  values obtained without the spin-contamination correction (red circles) and with the corrected approach (black circles). For comparison, the results of all-electron (AE) DFT calculations (ORCA software [38], PBE functional [39] and def2-TZVP basis set [40]) with the direct (red crosses) and UNO-corrected (black crosses) approaches are presented.

approximation of the two-particle spin density which is, otherwise, not directly available from DFT.

Due to spin polarization, the Kohn-Sham states of a paramagnetic system have different energies and different spatial distributions in the spin-up and spin-down channels. Therefore, the spin-spin ZFS is not entirely determined by the coupling between the half-filled states (denoted as  $\mathbf{d}^{I,I}$  in the energy level diagram in Fig. 1a, where a spin-triplet  $S = 1$  case is shown as a prototype example). Instead, it also contains non-vanishing collective contribution from the two-particle spin densities of single-/double- ( $\mathbf{d}^{I,II}$ ) and double-/double-occupied ( $\mathbf{d}^{II,II}$ ) states. Note that in the absence of spin polarization, the contributions from the spin-up and spin-down electrons of the same double-occupied orbital would cancel out due to the spin-dependent factor  $\chi_{m,n}$ .

The spin contamination manifests itself in unphysical spin-dipolar interaction which induces spurious 'on-site' terms in the two-particle spin density [4] entering  $\mathbf{d}^{I,II}$ . This can be nicely demonstrated by adopting the family of  $S = 1$  biradicals used in Ref. 4 as a reference system (see Fig. 1b). Here, the unpaired electrons are located at the opposite termini, so that the spin-spin ZFS *must* decrease according to the point-dipole approximation as the molecule gets longer and longer. This is, however, not the case as the unphysical 'on-site' contributions ( $\mathbf{d}_T^{I,II}$  in Fig. 1c, where the subscript is introduced to distinguish the triplet spin state) result in unrealistic  $D^{SS}$  values (Fig. 1d).

The considered biradicals represent a lucky case where

the physical and spin contamination driven parts of the magnetic dipolar coupling tensor are well-separated. Indeed, for the longer molecules, the coupling is completely described by  $\mathbf{d}_T^{I,I}$ , while  $\mathbf{d}_T^{I,II}$  is being entirely caused by spin contamination. In general, there is, however, no evidence that the spin contamination can be attributed only to selected terms in Eq. 3 or that it can be treated as an additive error. Therefore, it must be excluded in a more elaborate way. In this paper, we establish a systematic correction scheme based on the simple idea that the spin-contamination error in  $\mathbf{d}_{(m_S=S)}$  of the  $m_S = S$  high-spin state of a general  $S \geq 1$  system is one-to-one reflected by its  $m_S = S - 1$  state. In Fig. 1c, this is illustrated for the prototypical  $S = 1$  case. Its  $m_S = 0$  low-spin configuration is a single-Slater-determinant state and thus should be referred to as the broken-symmetry, BS, state. As a consequence, the average  $\bar{\mathbf{d}}_{(m_S=S-1)}$  among all the possible  $m_S = S - 1$  configurations restores the physical part while cancelling out the spin-contamination error completely (see also the discussion in the Supplemental Material (SM) [41]):

$$\bar{\mathbf{D}}^{SS} = \frac{\mathbf{d}_{(m_S=S)} - \bar{\mathbf{d}}_{(m_S=S-1)}}{2S - 1}, \quad (4)$$

Each of these  $m_S = S - 1$  configurations can be obtained by changing the occupation of one of the half-filled Kohn-Sham orbitals from spin-up to spin-down and subsequently performing the self-consistent field calculation. Note that the  $S$  dependent denominator in Eq. 4 is exactly the prefactor which relates the  $D$  values and the

energetic distance between the  $m_S = S$  and  $m_S = S - 1$  spin sublevels [41].

For an  $S = 1$  system, this follows directly from Fig. 1c. While showing no net spin, its  $m_S = 0$  BS state exhibits antiferromagnetic coupling between the spin-up and spin-down electrons occupying two half-filled orbitals, which leads to non-vanishing  $\mathbf{d}_{\text{BS}}^{1,1}$  (blue triangles in Fig. 1c). Thus, in a 'perfect' spin-triplet system, i.e. a system *without* spin contamination,  $\mathbf{d}_{\text{BS}} = -\mathbf{d}_{\text{T}}$  is expected. Consequently, when the spin-spin ZFS of a triplet system is defined as  $\bar{\mathbf{D}}^{\text{SS}} = (\mathbf{d}_{\text{T}} - \mathbf{d}_{\text{BS}})/2$ , the *physical*  $\mathbf{d}_{\text{T}}^{1,1}$  part is conserved, while the spin contamination error of the triplet and BS states cancel.

As an illustration, we apply the proposed strategy to the considered set of biradicals. Here and in the following, the spin-spin ZFS calculations [36] are based on the projector augmented wave (PAW) formalism [42] in combination with norm-conserving pseudopotentials [45], as implemented in a modified version of the GIPAW module of the Quantum ESPRESSO software [43, 44]. We used the PBE exchange-correlation functional [39], and a plane-wave (PW) basis set with 700 eV kinetic energy cutoff. We find that the corrected ZFS exhibits perfect agreement with the UNO-based all-electron DFT results (Fig. 1d). Most importantly, in contrast to the UNO approach, the established scheme is applicable for high-spin systems with periodic boundary conditions.

Subsequently, we apply the correction to the  $\text{NV}^-$  and  $\text{VV}^0$  defects in 4H-SiC, and the  $\text{NV}^-$  center in diamond. These spin-triplet defect centers are arguably among the most prominent solid-state spin qubits. Their ZFS is believed to be almost entirely caused by magnetic dipolar coupling and has been successfully treated with plane-wave pseudopotential DFT [10, 11, 32]. Some recent publications [36, 46, 47], however, argued that the reported agreement between the calculated and the measured ZFS profits from error cancellation due to incomplete treatment of the pseudized electron density. Indeed, as shown in Ref. [36], the resulting ZFS depends significantly on the technical parameters adopted for the pseudopotentials generation, unless the 'true' character of the wavefunction within the atomic core region is reconstructed. Such reconstruction can be achieved by the PAW method [42]. As pointed out by Ivády et al. [47], the fully PAW reconstructed ZFS of the spin-triplet centers in the SiC polytypes is, however, almost 30% larger than the values reported experimentally.

In diamond, there is only one magnetically distinct  $\text{NV}^-$  center. It can be aligned with one of the  $\langle 111 \rangle$  diagonals and always exhibits  $C_{3v}$  symmetry. In contrast, the hexagonal 4H polytype of SiC features a periodic sequence of quasicubic ( $k$ ) and hexagonal ( $h$ ) Si-C double layers along the crystal  $c$ -axis, offering inequivalent crystallographic positions and configurations for the defect pairs. Those  $\text{NV}^-$  and  $\text{VV}^0$  centers that are aligned with the hexagonal  $c$ -axis (the so-called *axial* pairs) have

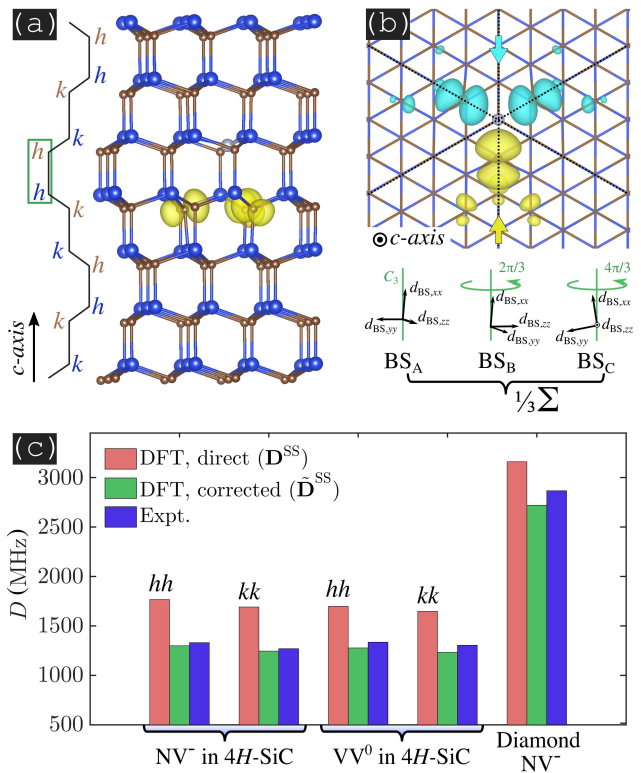


FIG. 2. Magnetic dipolar coupling driven ZFS of the  $\text{NV}^-$  and  $\text{VV}^0$  divacancy centers. (a) Crystal structure of 4H-SiC illustrating the two inequivalent Si (blue) and C (brown) lattice sites. Spin density of the  $\text{NV}^-$  center with the axial  $hh$  configuration is shown (yellow isosurface). (b) Spin density distribution in a selected BS state of the axial  $\text{NV}^-$  center and (below) schematic illustration of the three possible  $\mathbf{d}_{\text{BS}}$  tensor directions. The 'true low-spin'  $\bar{\mathbf{d}}_{(m_S=0)}$  tensor is defined as their average restoring the symmetry of the triplet state (in case of axial pairs,  $C_{3v}$ ). (c) The spin-spin  $D$  values obtained without (red) and with (green) the proposed spin contamination correction in comparison with the experimental data from Refs. [10, 11, 14, and 32] (blue).

$C_{3v}$  symmetry (see Fig. 2a). For all other orientations, the symmetry is lowered towards  $C_{1h}$ . Irrespective of the host material and the crystallographic position, the  $\text{NV}^-$  and  $\text{VV}^0$  defects share almost the same  $m_S = 1$  electronic structure with two unpaired electrons either populating a double degenerate  $e$  orbital (axial pairs) or slightly split  $a'$  and  $a''$  orbitals (basal pairs).

As shown in Fig. 2c and Table I, even for the axially symmetric  $\text{NV}^-$  and  $\text{VV}^0$  centers, the ZFS depend on the lattice site sensitively. Notably, our results for SiC reproduce the previously reported 30% discrepancy between the measured  $D$  values and  $D^{\text{SS}}$ , if directly calculated via Eq. 2. It should be also mentioned that the coupling of the two half-filled Kohn-Sham states (i.e., the  $\mathbf{d}_{\text{T}}^{1,1}$  term) explains in this case less than 70% of the measured value, rendering a spin-restricted approach (where

TABLE I. The spin-spin ZFS for the  $NV^-$  center in diamond, and  $NV^-$ ,  $VV^0$ ,  $V_{Si}^-$  centers in  $4H$ -SiC calculated without (second column,  $\mathbf{D}^{SS}$ ) and with (third column,  $\tilde{\mathbf{D}}^{SS}$ ) spin contamination correction in comparison with experiment.<sup>a</sup> The ZFS are provided as the  $D$  values ( $E$  values in parentheses if non-zero).

Defect/site	$\mathbf{D}^{SS}$	$\tilde{\mathbf{D}}^{SS}$	Expt.
axially symmetric $S = 1$ defects			
Diamond $NV^-$	3160.0	2720.7	2867
$NV^-/hh$	1767.3	1299.6	1331
$NV^-/kk$	1691.6	1245.7	1282
$VV^0/hh$	1698.5	1277.6	1336
$VV^0/kk$	1647.9	1234.4	1305
basal $S = 1$ defects			
$NV^-/hk$	1614.8 (159.4)	1127.4 (120.9)	1193 (104)
$NV^-/kh$	1733.6 (61.2)	1259.7 (8.9)	1328 (15)
$VV^0/hk$	1656.0 (42.2)	1219.2 (45.0)	1334 (19)
$VV^0/kh$	1592.3 (107.9)	1126.8 (89.3)	1222 (82)
axially symmetric $S = 3/2$ defects			
$V_{Si}^-/h$	26.5	1.8	2.6
$V_{Si}^-/k$	47.4	38.5	35.0

<sup>a</sup> Experimental values taken from Ref. 32 (diamond), Refs. 10 and 11 ( $NV^-$  in SiC), Ref. 14 ( $VV^0$ ), and from Ref. 22 ( $V_{Si}^-$ ). The calculations performed using 512-atom (diamond) and 432-atom ( $4H$ -SiC) supercells with shifted  $2 \times 2 \times 2$   $k$ -point grids.

the same wavefunctions are used for spin-up and spin-down) to be insufficient. The  $\mathbf{d}_T^{I,II}$  and  $\mathbf{d}_T^{II,II}$  terms are, thus, significant for  $NV^-$  and must be retained in a systematic manner. In the following, we show that this can be accomplished by using the proposed methodology.

In contrast to the biradicals considered above (Fig. 1), the unpaired electrons of the *axial*  $NV^-$  or  $VV^0$  center are equally distributed among the three carbon dangling bonds surrounding the vacancy (cf. Fig. 2a). Thus, in a  $m_S = 0$  configuration, the spin-up electron can localize at one of these dangling bonds, while the spin-down electron is being shared by the other two adjacent carbon atoms. As illustrated in Fig. 2b, this provides three symmetry-reduced BS states of the axial defect. Thus, in order to apply Eq. 4 to the ZFS of  $NV^-$  and  $VV^0$ , we define the  $\tilde{\mathbf{d}}_{(m_S=0)}$  tensor as the  $C_{3v}$  symmetrized average of the three resulting BS tensors.

Figure 2c demonstrates that the spin decontamination applied in this way removes the overestimation and brings the calculated ZFS ( $\tilde{\mathbf{D}}^{SS}$ ) in almost perfect agreement with the measured  $D$  values. The improvement is especially decisive for the spin qubits in SiC. Note that a part of the remaining discrepancies ( $< 100$  MHz) can be attributed to second-order contributions to the ZFS due to spin-orbit coupling [48].

The same procedure can be applied in case of the basal

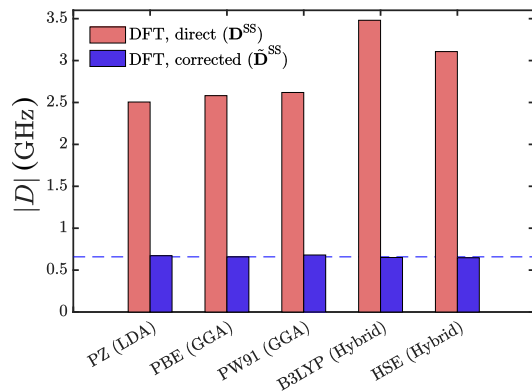


FIG. 3. Spin-spin ZFS (the absolute value of  $D$ ) of the  $C_5H_{10}$  spin-triplet biradical (from the set considered in Fig. 1) calculated with different exchange-correlation functionals: PZ [49], PBE, PW91 [50], B3LYP [51] and HSE [52]. Horizontal dashed line indicating the  $\tilde{\mathbf{D}}^{SS}$  value obtained with the PBE functional is provided as a guide for the eye.

pairs in SiC. From Table I it can be seen that these spin qubits suffer from the spin contamination to the same extent as their axially symmetric counterparts. Averaging of their three no-longer equivalent BS configurations provides improved estimates for  $D$ , and also reasonable values for the rhombicity parameter  $E$ . Finally, we show that the proposed approach can be successfully used for higher spin qubits, i.e. the  $V_{Si}^-$  centers in  $4H$ -SiC that possess a  $S = 3/2$  ground state. Notably, the  $D$  value of  $V_{Si}^-$  at the  $h$  site is found to manifest enormous spin contamination error, which is eliminated by our correction scheme (cf. Table I). Because of an exceptional accuracy provided by our approach, the reported results can be considered as a solid contribution that supports the assignment of the spectroscopic fingerprints observed in  $4H$ -SiC as  $NV^-$ ,  $VV^0$  and  $V_{Si}^-$  centers.

To summarize, in the present work we propose an efficient scheme to eliminate spin contamination in magnetic dipolar coupling. It allows us to identify the spin contamination of the two-electron density as a highly relevant source of discrepancy between measured and calculated ZFS of high-spin defects in semiconductors. This discrepancy can be lifted by calculating the difference of  $m_S = S$  and  $m_S = S - 1$  magnetic dipolar coupling tensors. This scheme is robust with respect to the exchange-correlation functional (see Fig. 3). In particular, it compensates the increased extent of spin contamination associated with the introduction of a fraction of exact Hartree-Fock exchange in hybrid functionals [5, 53, 54]. This opens up the possibility to use either hybrid functionals or (semi)local (LDA and GGA) functionals while reaching the same level of accuracy for the spin-spin ZFS. The proposed correction will be also beneficial for an accurate description of magnetic dipolar interaction between *distant* spin centers, e.g., for modelling

a qubit coupled to a spin-bath [55–57] or a solid-state spin probe coupled to surface electron spins [58].

Numerical calculations were performed using grants of computer time from the Paderborn Center for Parallel Computing (PC<sup>2</sup>) and the HLRS Stuttgart. The Deutsche Forschungsgemeinschaft (DFG) is acknowledged for financial support via the priority program SPP 1601 and the Transregional Collaborative Research Center TRR 142 (project number 231447078).

- 
- [1] A. Abragam and B. Bleaney, *Electron Paramagnetic Resonance of Transition Ions* (Oxford University Press, Oxford, 2013).
- [2] J. E. Harriman, *Theoretical Foundations of Electron Spin Resonance* (Academic press, New York, 1978).
- [3] S. Sinnecker, and F. Neese, Spin-spin contributions to the zero-field splitting tensor in organic triplets, carbenes and biradicals—a density functional and *ab initio* study, *J. Phys. Chem. A* **110**, 12267–12275 (2006).
- [4] P. Jost and C. van Wüllen, Why spin contamination is a major problem in the calculation of spin-spin coupling in triplet biradicals, *Phys. Chem. Chem. Phys.*, **15**, 16426–16427 (2013).
- [5] J. Baker, A. Scheiner, and J. Andzelm, Spin contamination in density functional theory, *Chem. Phys. Lett.* **216**, 380–388 (1993).
- [6] N. Ferré, N. Guihéry, and J. P. Malrieu, J. P. (2015). Spin decontamination of broken-symmetry density functional theory calculations: deeper insight and new formulations. *Phys. Chem. Chem. Phys.*, **17**, 14375–14382.
- [7] S.-I. Sato, T. Narahara, Y. Abe, Y. Hijikata, T. Umeda, and T. Ohshima, Formation of nitrogen vacancy centers in 4H-SiC and their near infrared photoluminescence properties, *J. Appl. Phys.* **126**, 083105 (2019).
- [8] H. J. von Bardeleben, J. L. Cantin, A. Csóré, A. Gali, E. Rauls, and U. Gerstmann, NV centers in 3C, 4H, and 6H silicon carbide: A novel platform for solid-state qubits and nanosensors, *Phys. Rev. B* **94**, 121202(R) (2016).
- [9] S. A. Zargaleh, H. J. von Bardeleben, J. L. Cantin, U. Gerstmann, S. Hameau, B. Eble, and W. Gao, Electron paramagnetic resonance tagged high-resolution excitation spectroscopy of NV-centers in 4H-SiC, *Phys. Rev. B* **98**, 214113 (2018).
- [10] A. Csóré, H. J. Von Bardeleben, J. L. Cantin, and A. Gali, Characterization and formation of NV centers in 3C, 4H, and 6H SiC: An *ab initio* study, *Phys. Rev. B* **96**, 085204 (2017).
- [11] H. J. Von Bardeleben, J. L. Cantin, A. Csóré, A. Gali, E. Rauls, and U. Gerstmann, NV centers in 3C, 4H, and 6H silicon carbide: A variable platform for solid-state qubits and nanosensors, *Phys. Rev. B* **94**, 121202 (2016).
- [12] J. F. Wang, F. F. Yan, Q. Li, Z. H. Liu, H. Liu, G. P. Guo, L. P. Guo, X. Zhou, J. M. Cui, J. Wang, and Z. Q. Zhou, Coherent control of nitrogen-vacancy center spins in silicon carbide at room temperature, arXiv preprint arXiv:1909.12481 (2019).
- [13] W. F. Koehl, B. B. Buckle, F. J. Heremans, G. Calusine, and D. D. Awschalom, Room temperature coherent control of defect spin qubits in silicon carbide, *Nature* **479**, 84 (2011).
- [14] A. L. Falk, B. B. Buckley, G. Calusine, W. F. Koehl, V. V. Dobrovitski, A. Politi, C. A. Zorman, P. X.-L. Feng, and D. D. Awschalom, Polytype control of spin qubits in silicon carbide, *Nat. Commun.* **4**, 1819 (2013).
- [15] C. F. de las Casas, D. J. Christle, J. Ul Hassan, T. Oshima, N. T. Son, and D. Awschalom, Stark tuning and electrical charge state control of single divacancies in silicon carbide, *Appl. Phys. Lett.* **111**, 262403 (2017).
- [16] D. J. Christle, P. V. Klimov, C. F. de la Casas, K. Szasz, V. Ivady, V. Jokubavicius, J. ul Hassan, M. Syväjärvi, W. F. Koehl, T. Oshima, N. T. Son, E. Janzen, A. Gali, and D. D. Awschalom, Isolated Spin Qubits in SiC with a High-Fidelity Infrared Spin-to-Photon Interface, *Phys. Rev. X* **7**, 021046 (2017).
- [17] H. Seo, A. L. Falk, P. V. Klimov, K. C. Miao, G. Galli, and D. D. Awschalom, Quantum decoherence dynamics of divacancy spins in silicon carbide, *Nat. Commun.* **7**, 12935 (2016).
- [18] O. V. Zwier, D. O’Shea, A. R. Onur, and C. H. van der Wal, All-optical coherent population trapping with defect spin ensembles in silicon carbide, *Sci. Rep.* **5**, 10931(2015).
- [19] D. Simin, V. A. Soltamov, A. V. Poshakinskiy, A. N. Anisimov, R. A. Babunts, D. O. Tolmachev, E. N. Mokhov, M. Trupke, S. A. Tarasenko, A. Sperlich, P. G. Baranov, V. Dyakonov, and G. V. Astakhov, *Physical Review X* **6**, 031014 (2016).
- [20] M. Widmann, S.-Y. Lee, T. Rendler, N. T. Son, H. Fedder, S. Paik, L.-P. Yang, N. Zhao, S. Yang, I. Booker, A. Denisenko, M. Jamali, S. A. Momenzadeh, I. Gerhardt, T. Ohshima, A. Gali, E. Janzén and J. Wrachtrup, *Nature Materials* **14**, 164–168 (2015).
- [21] H. Kraus, V.A. Soltamov, D. Riedel, S. Váth, F. Fuchs, A. Sperlich, P.G. Baranov, V. Dyakonov, G.V. Astakhov, *Nature Physics* **10**, 157 (2014).
- [22] V. Ivády, J. Davidsson, N.T. Son, T. Ohshima, I.A. Abrikosov, A. Gali, *Physical Review B* **96**, 161114(R) (2017).
- [23] M. W. Doherty, N. B. Manson, P. Delaney, F. Jelezko, J. Wrachtrup, and L. C. L. Hollenberg, The nitrogen vacancy colour center in diamond, *Phys. Rep.* **528**, 1 (2013).
- [24] D. D. Awschalom, R. Hanson, J. Wrachtrup, and B. B. Zhou, Quantum technologies with optically interfaced solid-state spins, *Nat. Photon.* **12**, 516 (2018).
- [25] N. Y. Yao, L. Jiang, A. V. Gorshkov, P. C. Maurer, G. Giedke, J. I. Cirac, and M. D. Lukin, Scalable architecture for a room temperature solid-state quantum information processor, *Nat. Commun.* **3**, 800 (2012).
- [26] B. Hensen, H. Bernien, A. E. Dréau, A. Reiserer, N. Kalb, M. S. Blok, J. Ruitenberg, R. F. L. Vermeulen, R. N. Schouten, C. Abellán, W. Amaya, V. Pruneri, M. W. Mitchell, M. Markham, D. J. Twitchen, D. Elkouss, S. Wehner, T. H. Taminiau, and R. Hanson, Loophole-free Bell inequality violation using electron spins separated by 1.3 kilometres, *Nature* **526**, 682 (2015).
- [27] K. Arai, C. Belthangady, H. Zhang, N. Bar-Gill, S. J. DeVience, P. Cappellaro, A. Yacoby, and R. L. Walsworth, Fourier magnetic imaging with nanoscale resolution and compressed sensing speed-up using electronic spins in diamond, *Nat. Nanotechnol.* **10**, 859 (2015).
- [28] F. Dolde, H. Fedder, M. W. Doherty, T. Nöbauer, F. Rempp, G. Balasubramanian, T. Wolf, F. Reinhard, L.

- C. L. Hollenberg, F. Jelezko, and J. Wrachtrup, Electric-field sensing using single diamond spins, *Nat. Phys.* **7**, 459 (2011).
- [29] G. Kucsko, P. C. Maurer, N. Y. Yao, M. Kubo, H. J. Noh, P. K. Lo, H. Park, and M. D. Lukin, Nanometre-scale thermometry in a living cell, *Nature* **500**, 54 (2013).
- [30] M. W. Doherty, V. V. Struzhkin, D. A. Simpson, L. P. McGuinness, Y. Meng, A. Stacey, T. J. Karle, R. J. Hemley, N. B. Manson, L. C. L. Hollenberg, and S. Prawer, Electronic Properties and Metrology Applications of the Diamond NV<sup>-</sup> Center Under Pressure, *Phys. Rev. Lett.* **112**, 047601 (2014).
- [31] M. S. J. Barson, P. Peddibhotla, P. Ovarthaiyapong, K. Ganesan, R. L. Taylor, M. Gebert, Z. Mielens, B. Koslowski, D. A. Simpson, L. P. McGuinness, J. McCallum, S. Prawer, S. Onoda, T. Ohshima, A. C. B. Jayich, F. Jelezko, N. B. Manson, and M. W. Doherty, Nanomechanical sensing using spins in diamond, *Nano Lett.* **17**, 1496 (2017).
- [32] V. Ivaády, T. Simon, J. R. Maze, I. A. Abrikosov, and A. Gali, Pressure and temperature dependence of the zero-field splitting in the ground state of NV centers in diamond: A first-principles study, *Phys. Rev. B* **90**, 235205 (2014).
- [33] R. McWeeny, and Y. Mizuno, The density matrix in many-electron quantum mechanics II. Separation of space and spin variables; spin coupling problems, *Proc. R. Soc. London A* **259**, 554-577 (The Royal Society, 1961).
- [34] S. Schmitt, P. Jost, and C. van Wüllen, Zero-field splittings from density functional calculations: Analysis and improvement of known methods. *J. Chem. Phys.* **134**, 194113 (2011).
- [35] M. J. Rayson, and P. R. Briddon, First principles method for the calculation of zero-field splitting tensors in periodic systems, *Phys. Rev. B* **77**, 035119 (2008).
- [36] T. Biktagirov, W. G. Schmidt, and U. Gerstmann, Calculation of spin-spin zero-field splitting within periodic boundary conditions: Towards all-electron accuracy, *Phys. Rev. B* **97**, 115135 (2018).
- [37] Z. Bodrog, and A. Gali, The spin-spin zero-field splitting tensor in the projector-augmented-wave method, *J. Phys.: Cond. Mat.* **26**, 015305 (2013).
- [38] F. Neese, The ORCA program system, *Wiley Interdiscip. Rev.: Comput. Mol. Sci.* **2**, 73 (2012).
- [39] J. P. Perdew, K. Burke, and M. Ernzerhof, Generalized gradient approximation for the exchange-correlation hole of a many-electron system, *Phys. Rev. Lett.* **77**, 3865 (1996).
- [40] F. Weigend and R. Ahlrichs, Balanced basis sets of split valence, triple zeta valence and quadruple zeta valence quality for H to Rn: Design and assessment of accuracy. *Phys. Chem. Chem. Phys.*, **7**, 3297-3305 (2005).
- [41] See Supplemental Material at <http://link.aps.org/supplemental/10.1103/PhysRevResearch.2.022024> for a discussion of the  $S > 1$  case.
- [42] P. E. Blöchl, Projector augmented-wave method, *Phys. Rev. B* **50**, 17953 (1994).
- [43] P. Giannozzi, O. Andreussi, T. Brumme, O. Bunau, M. Buongiorno Nardelli, M. Calandra, R. Car, C. Cavazzoni, D. Ceresoli, M. Cococcioni, N. Colonna, I. Carnimeo, A. Dal Corso, S. de Gironcoli, P. Delugas, R. A. DiStasio Jr, A. Ferretti, A. Floris, G. Fratesi, G. Fugallo, R. Gebauer, U. Gerstmann, F. Giustino, T. Gorni, J. Jia, M. Kawamura, H.-Y. Ko, A. Kokalj, E. Kkbenli, M. Lazzeri, M. Marsili, N. Marzari, F. Mauri, N. L. Nguyen, H.-V. Nguyen, A. Otero-de-la-Roza, L. Paulatto, S. Poncé, D. Rocca, R. Sabatini, B. Santra, M. Schlipf, A. P. Seitsonen, A. Smogunov, I. Timrov, T. Thonhauser, P. Umari, N. Vast, X. Wu and S. Baroni, Advanced capabilities for materials modelling with Quantum ESPRESSO, *J. Phys.: Cond. Mat.* **29**, 465901 2017.
- [44] P. Giannozzi, S. Baroni, N. Bonini, M. Calandra, *et al.*, QUANTUM ESPRESSO: a modular and open-source software project for quantum simulations of materials, *J. Phys.: Cond. Mat.* **21**, 395502 2009.
- [45] N. Troullier, and J. L. Martins, Efficient pseudopotentials for plane-wave calculations, *Phys. Rev. B* **43**, 1993 (1991).
- [46] H. Seo, H. Ma, M. Govoni, and G. Galli, Designing defect-based qubit candidates in wide-gap binary semiconductors for solid-state quantum technologies, *Phys. Rev. Mater.* **1**, 075002 (2017).
- [47] V. Ivády, I. A. Abrikosov, and A. Gali, First principles calculation of spin-related quantities for point defect qubit research, *NPJ Comput. Mater.* **4**, 76 (2018).
- [48] T. Biktagirov and U. Gerstmann, Spin-orbit driven electrical manipulation of the zero-field splitting in high-spin centers in solids, *Phys. Rev. Research* **2**, 023071 (2020)
- [49] J. P. Perdew and A. Zunger, Self-interaction correction to density-functional approximations for many-electron systems, *Phys. Rev. B* **23**, 5048 (1981).
- [50] J. P. Perdew and Y. Wang, Accurate and simple analytic representation of the electron-gas correlation energy, *Phys. Rev. B* **46**, 6671 (1992).
- [51] P. J. Stephens, F. J. Devlin, C. F. Chabalowski, M. J. Frisch, Ab Initio Calculation of Vibrational Absorption and Circular Dichroism Spectra Using Density Functional Force Fields, *J. Phys. Chem.* **98**, 11623 (1994).
- [52] J. Heyd, G. E. Scuseria, M. Ernzerhof, Hybrid functionals based on a screened Coulomb potential, *J. Phys. Chem.* **118**, 8207 (2003); J. Heyd, G. E. Scuseria, M. Ernzerhof, *J. Phys. Chem.* **124**, 219906 (2006).
- [53] F. Neese, Calculation of the zero-field splitting tensor on the basis of hybrid density functional and Hartree-Fock theory, *J. Chem. Phys.* **127**, 164112 (2007).
- [54] A. S. Menon and L. Radom, Consequences of Spin Contamination in Unrestricted Calculations on Open-Shell Species: Effect of Hartree-Fock and Møller-Plesset Contributions in Hybrid and Double-Hybrid Density Functional Theory Approaches, *J. Phys. Chem A* **112**, 13225-13230 (2008).
- [55] C. Belthangady, N. Bar-Gill, L. M. Pham, K. Arai, D. Le Sage, P. Cappellaro, and R. L. Walsworth, Dressed-state resonant coupling between bright and dark spins in diamond, *Phys. Rev. Lett.* **110**, 157601 (2013).
- [56] M. W. Doherty, C. A. Meriles, A. Alkauskas, H. Fedder, M. J Sellars, and N. B. Manson, Towards a room-temperature spin quantum bus in diamond via electron photoionization, transport, and capture, *Phys. Rev. X* **6**, 041035 (2016).
- [57] E. van Oort, P. Stroomeer, and M. Glasbeek, Low-field optically detected magnetic resonance of a coupled triplet-doublet defect pair in diamond, *Phys. Rev. B* **42**, 8605 (1990).
- [58] A. Sushkov, I. Lovchinsky, N. Chisholm, R. L. Walsworth, H. Park, and M. D. Lukin, Magnetic sensing and imaging using interactions between surface electron

spins and solid state spins *U.S. Patent No. 9,891,297*  
(2018).